Optical response of tunable terahertz plasmon in a grating-gated graphene transistor*

Bo Yan(闫博)[1,2,3], Jingyue Fang(方靖岳)[2,†], Shiqiao Qin(秦石乔)[2], Yongtao Liu(刘永涛)[3], Li Chen(陈力)[1], Shuang Chen(陈爽)[1], Renbing Li(李仁兵)[1], and Zhen Han(韩震)[1]

[1] *China Aerodynamics Research and Development Center, Mianyang* 621000, *China*
[2] *College of Science, National University of Defense Technology, Changsha* 410073, *China*
[3] *Key Laboratory of Nanodevices and Applications, Suzhou Institute of Nano-tech and Nano-bionics, Chinese Academy of Sciences, Suzhou* 215123, *China*

(Received 17 April 2017; revised manuscript received 10 June 2017; published online 27 July 2017)

Tunable terahertz plasmon in a graphene-based device with a grating serving as a top gate is studied. Transmission spectra exhibit a distinct peak in the terahertz region when the terahertz electric field is perpendicular to the grating fingers. Our results show that the extinction in the transmission of single-layer graphene shields beyond 80%. Electronic results further show that the graphene plasmon can be weakly adjusted by tuning the gate voltage. Theoretical calculation also implies that the plasmon frequency of graphene can fall into the terahertz region of 1–2 THz by improving the sustaining ability and capacitance of the top gate.

Keywords: graphene plasmon, Lorentz, terahertz time-domain spectroscopy, electrical measurement

PACS: 78.67.Wj, 87.50.U, 72.80.Vp, 52.40.−w **DOI:** 10.1088/1674-1056/26/9/097802

1. Introduction

Graphene plasmon is attracting increased research attention because of their potential applications in technology, especially in optoelectronics.[1–3] Many theoretical studies have focused on terahertz graphene plasmon[4–6] because it exhibits many unusual behaviors, such as high wave velocity and long propagation distance.[4,7,8] Engineering a tunable graphene plasmon device is one of the key experiment tasks to determine their superior characteristics. Tunable terahertz plasmon in graphene ribbons/resonant electromagnetic (EM) cavities has recently been investigated to develop plasmon-based terahertz devices. However, the coupling between graphene and incident terahertz wave is relatively weak.[9,10]

The adoption of metallic grating and resonant cavity is one of the best solutions, and such a scheme has been studied in our previous paper.[6,11] The upper grating serves as a superior coupler to excite graphene plasmon.[6,11,12] The interaction between graphene plasmon and EM wave can be enhanced by a Fabry–Pérot cavity.[6,11,13] The relation between graphene plasmon frequency and the grating width has also been quantitatively analyzed.[11]

This study investigates the voltage-tunable terahertz plasmon in a grating-coupled two-dimensional electron density (2DEG) embedded in a Fabry–Pérot cavity, using the terahertz time-domain spectroscopy (THz-TDS). Transmission theoretical calculation on the graphene plasmon agrees well with the experimental results. Methods to enhance the tunability of the prepared device are discussed in the next sections.

2. Experiments

Three main building blocks were involved in this device, a graphene sheet, a Fabry–Pérot cavity, and a grating, as shown in Fig. 1(a). The graphene was synthesized by chemical vapor deposition (CVD) method under low pressure and high temperature. After that, it was transferred onto a silicon substrate (THz permittivity, $\varepsilon_1 = 11.9$) with a 300-nm oxide layer (THz permittivity, $\varepsilon_2 = 4$) by using the PMMA transfer method. Raman measurements were performed in the as-prepared sample. Results show that the transferred graphene is single layered with high quality[14,15] (see Fig. 1(b)). A thin film of Al_2O_3 was deposited on the sample by atomic layer deposition (ALD)[16] subsequently, whose chamber temperature was set to 140 °C and 280 rounds of deposition were carried out. The thickness of Al_2O_3 film deposited on graphene was about 25 nm. These three elements (Al_2O_3/SiO_2/Si) introduced above make up the main body of the cavity. Next, the 100-nm thick gold grating gate, coupling the terahertz EM wave to the grapheme plasmon and regulating the electronic density of graphene, was fabricated on top of the Al_2O_3 layer. The grating constant L was 8.7 μm when the length of the individual gold finger W was 4.7 μm (see Fig. 1(c)). The source and drain electrodes were produced simultaneously when the

*Project supported by the National Natural Science Foundation of China (Grant No. 11272337), the Research Project of National University of Defense Technology, China (Grant No. ZK16-03-34), the Natural Science Foundation of Hunan Province, China (Grant No. 2016JJ3021), and the Open Project of Key Laboratory of Nanodevices and Applications, Suzhou Institute of Nano-tech and Nano-bionics, Chinese Academy of Sciences (Grant No. 15ZS03).

†Corresponding author. E-mail: fjynudt@aliyun.com

© 2017 Chinese Physical Society and IOP Publishing Ltd

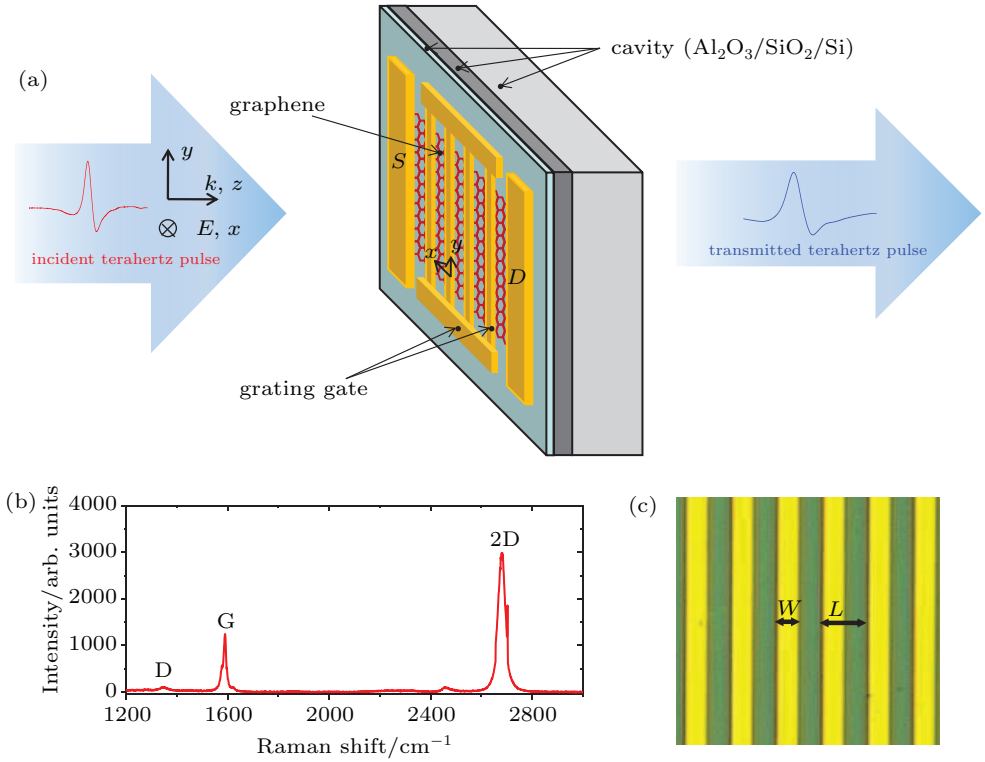


Fig. 1. (color online) (a) Schematic structure of the device and the coordinate notation for transmission measurement. (b) Measured Raman spectrum of the transferred monolayer graphene on top of the Si/SiO_2 substrate. (c) The optical photo of the grating gate.

grating gate was prepared. Besides, the device was encapsulated using a chip carrier with 24 pins. The overall thickness and the total functional area of the sample were $D_1 = 190$ μm and $S_1 = 4 \times 4$ mm^2, respectively. Finally, the THz-TDS technique allowed us to obtain the transmission spectrum at different gate voltages. The incident light polarized along the grid fingers, as shown in Fig. 1(a).

3. Results and discussion

Transmission of the bare cavity and the grating-coupled graphene plasmon device are shown in Fig. 2(a). The bare cavity is an insulator with constant transmission level in the THz region. However, the transmission spectra measured on the graphene device with resonant cavity shows that a prominent peak locates at 1.511 THz. This phenomenon implies that THz absorption is observably affected by graphene. Thus, extinction spectra $(1-T/T_0)$ for grating devices with $V_{TG} = -0.8$ V, 0 V, 0.8 V were then investigated.

To compare with the experimental data, we calculate $(1-T/T_0)$ of the graphene device theoretically by[11]

$$1 - T/T_0 = 1 - \frac{1}{|1 + Z_0\sigma(\omega)/(1+n_s)|^2}, \tag{1}$$

where T_0 and T are the transmissions passing through the bare cavity and the sample with the graphene, respectively. Z_0 is the vacuum impedance, and n_s is the effective refractive index of the substrate. The solid curves in Fig. 2(b) are fitting results according to Eq. (1) and the Lorentz conductivity. We use Lorentz conductivity for the graphene layer as[10,11]

$$\sigma_{2D} = \mathrm{i}\sqrt{\frac{n}{\pi}}\frac{e^2 v_F \omega}{\hbar(\omega_p^2 - \omega^2 + \mathrm{i}\omega\Gamma_p)}, \tag{2}$$

where ω is the radian frequency of the incident terahertz light, n is the carrier density, and Γ_p is the plasmon resonance width. The resonance frequency is given by[10,11]

$$\omega_p(q) = 2\pi f_p = \sqrt{\frac{8E_F\sigma_{uni}k_G}{\hbar\varepsilon}}, \tag{3}$$

where ε and k_G are effective dielectric constant and plasmon wave vector, respectively. The $\sigma_{uni} = \pi e^2/2h$ is the well-known optical conductivity, and the Femi energy is given by $E_F = hv_F(\pi n)^{1/2}$, $v_F = 1 \times 10^6$ m/s. If the sample is irradiated vertically by the light, the plasmon wave vector is determined by $k_G = m\pi/W$ with $m = 1, 2, 3, \ldots$[11,17]

The corresponding solid curves in Fig. 2(b) are fitting results according to Eqs. (1)–(3) with n and Γ_p as two fitting parameters. Three prominent features for the data are presented in Fig. 2(b). First, the plasmon resonance width of the as-prepared sample is approximately 3.5 THz, whereas the carrier density n ranges from 7.16×10^{12} cm^{-2} to 8.36×10^{12} cm^{-2}. Second, an obvious blue shift of the plasmon resonance frequency with decreasing top-gate voltage is observed: resonance frequencies are located at 1.523 THz, 1.511 THz, and

1.506 THz for voltage of 0.8 V, 0 V, and −0.8 V, respectively. Using a larger range of effective top-gate voltage, terahertz resonance in 1–2 THz can be straightforwardly achieved (see Fig. 5). Third, the light–plasmon coupling in graphene is remarkably strong; transmission extinction at the plasmon resonance for $V_{TG} = 0$ V is more than 80%. A higher extinction can be achieved readily by enlarging the top-gate voltage V_{TG}.

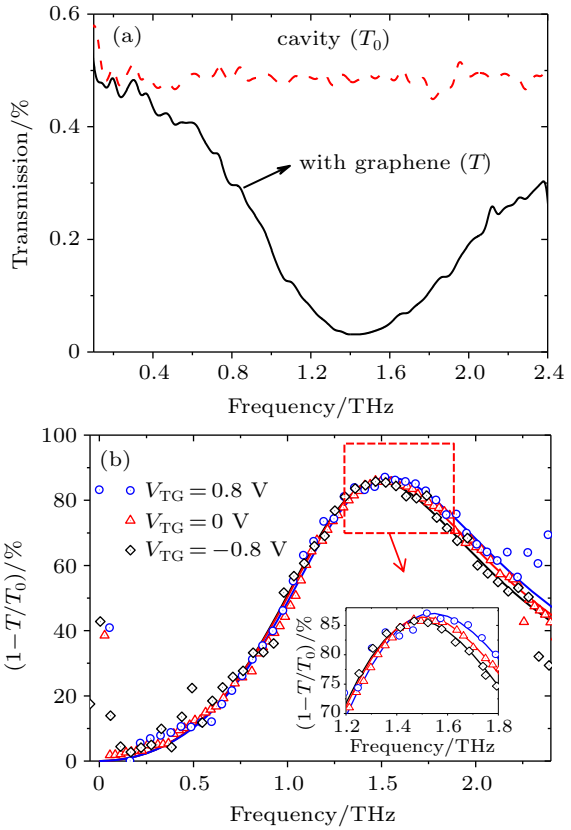


Fig. 2. (color online) (a) Transmission spectra of the bare cavity (T_0) and the device with graphene (T). (b) Extinction in transmission, $1-T/T_0$, in the graphene plasmonic device as gate voltage V_G are −0.8, 0, and 0.8. The solid lines are fitting curves. Inset shows partial enlarged details inside the red-dashed box. The maximal transmission extinction is approximately 85%.

The electrical properties of the engineered graphene plasmon device are discussed by performing a fullest direct current (DC) measurement. Figure 3 shows the equivalent current model in the DC measurement. First, the output character is measured to obtain the device resistance (see Figs. 3(a) and 4(a)). The channel current of the graphene device is found to be linear with the output voltage V_{DS}, and the output resistance is proved to be a constant of 1639 Ω. Second, the leakage character of the fabricated graphene plasmon device is obtained in Figs. 3(b) and 4(b). In the measurement, the source and drain electrodes are linked to the ground. Figure 3(b) shows the leakage measurement equivalent model. The top-gate structure can be regarded as a parallel between the top-gate capacitance C_x and junction resistance R_G because of the top-gate leakage. In DC measurement, the current can only flow through the resistance R_G. The leakage current results I_{G1} and I_{G2} show an almost perfect symmetry to the origin of coordinates (Fig. 4(b)). The total leakage current is $I_G = I_{G1} + I_{G2} \approx 1.5$ μA when $V_{TG} = 0.85$ V. Thus, the junction resistance R_G is approximately 0.6 MΩ, far less than that of small-size top-gate media. Meanwhile, the value of I_{G1} is almost the same as that of I_{G2}. Assuming two graphene channel resistances close to the source and drain electrodes are equal, $R_S \approx R_D$.

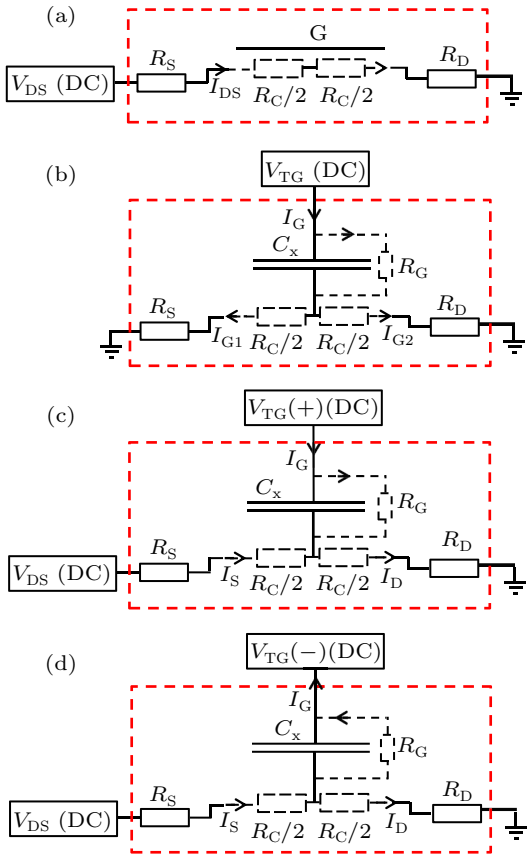


Fig. 3. (color online) Equivalent current models. Here, R_S and R_D are considered as contact resistances in the source and drain electrodes, respectively. Graphene channel resistance is regarded as two parts close to the source and drain electrodes. Both resistances are set equally to calculate easily, and C_x and R_G are the top-gate capacitance and resistance, respectively. (a) Output-character measurement model. (b) Leak current measurement model. Panels (c) and (d) are transfer-characters measurements for positive and negative voltage, respectively.

Third, our double DC measurement of the prepared graphene device for different top-gate voltages will explicitly indicate the transfer character, as shown in Figs. 3(c), 3(d), and 4(c). From the values of I_D, I_S, and I_G extracted from the DC measurement (inset in Fig. 4(c)), the actual top-gate voltage V_G set on the capacitance C_x at different gate voltages can be obtained in Fig. 4(c). Here, $V_G = V_{TG} - V$ (see Figs. 3(c) and 3(d)), with graphene channel voltage $V = I_D(R_D + R_C/2) = V_{DS} - I_S(R_S + R_C/2)$. To further simplify, $R_S + R_C/2 = R_D + R_C/2 = V_{DS}/(I_S + I_D)$, $V = V_{DS}I_D/(I_S + I_D)$. As a result, $V_G = V_{TG} - V_{DS}I_D/(I_S + I_D)$, and the actual channel current due to the graphene carrier can be expressed by $I_{DS} = V_0/R_t$, where the whole device resistance R_t

can be given by $R_t = R_D + R_S + R_C = 2V_{DS}/(I_S + I_D)$, and V_0 is set as 10 mV. The theoretical fitting for our transfer characteristic data will be discussed below. The carrier concentration (electrons or holes) in the graphene channel regions n related to the residual carrier concentration n_0 and the Dirac-point voltage V_{Dirac} can be approximated by $n = \sqrt{n_0^2 + n_1^2}$, $V_G - V_{Dirac} = en_1/C_x + \hbar v_F\sqrt{\pi n_1}/e$,[18] where C_x and n_0 can be set as 122.4 nF/cm^2 and 1×10^{12} cm^{-2} in our fitting model, respectively. The total device resistance R_t is given by $R_t = R_{contact} + L/(We\mu n)$,[18] where the contact resistance is $R_{contact} = R_S + R_D$ and μ represents the mobility. Finally, the channel current is given by $I_{DS} = V_0/R_t$. The measured I_{DS} against V_G (symbols) along with the fitting results (solid lines) is shown in Fig. 4(c). Then, the relevant parameters can be extracted: $V_{Dirac} = -10.5$ V, $\mu = 1500$ cm^2·V^{-1}·s^{-1} and $R_{contact} = 770\ \Omega$.

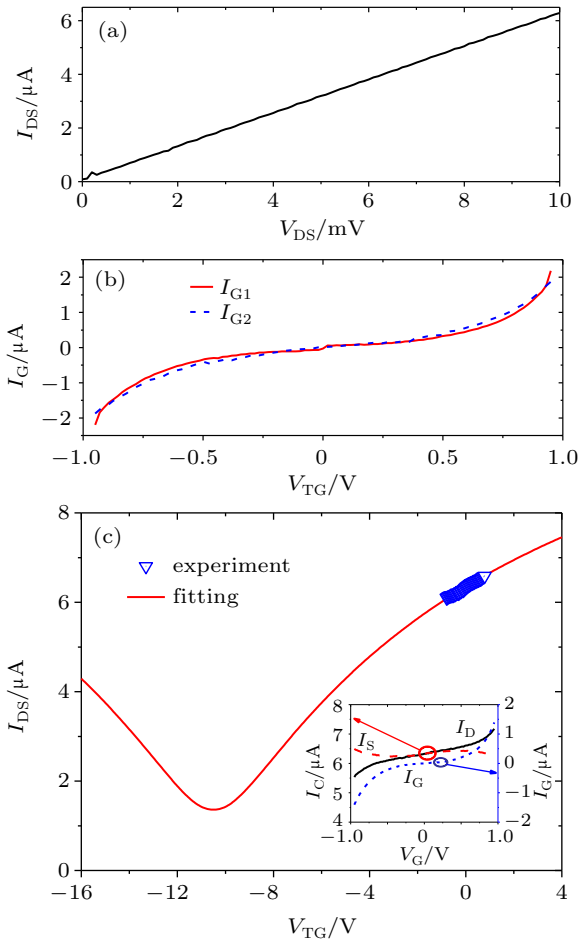


Fig. 4. (color online) (a) Output characteristic curve. (b) Leak current curve (red solid line (I_{G1}) and blue dashed line (I_{G2})). (c) Transfer characteristic curve of experimental and theoretical fitting results. Inset shows the channel and leakage results measured at the same time.

However, the variation range of the graphene plasmon frequency is very small, as shown in Fig. 5. The calculating parameters were set as the same as those in Fig. 4(c). In our experiments, tiny top-gate voltage range was applied to the device. Otherwise, when the larger top-gate voltage is applied to modulate the carrier density of the graphene channel, the leakage current can reach up more than 1.5 μA (see Fig. 4(b)). Therefore, the top-gate voltage can only be set as small as possible to avoid the large leakage current to breakdown the top-gate capacitance. Two aspects should be considered to develop a device with a larger plasmon frequency range. First, defects of the top-gate media can be decreased by enlarging the growth temperature of ALD and applying the graphene prepared using molecular beam epitaxy (MBE).[19] As a result, the sustaining capability of the top-gate media can be improved directly. Second, the thickness and permittivity of top-gate dielectric layers can be optimized to enlarge its capacitance. Consequently, the range of graphene plasmon frequency can also be expanded (see the inset of Fig. 5).

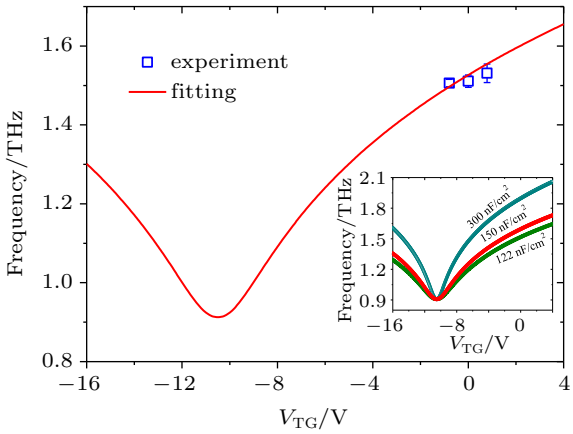


Fig. 5. (color online) Experiment and theoretical frequency character of the prepared graphene plasmon device as a function of the top-gate voltage. Inset shows the graphene plasmon frequencies calculated at different top-gate dielectric capacitances.

4. Conclusion and perspectives

In summary, a tunable graphene plasmon device was fabricated with an Al_2O_3 gate dielectric on its surface by ALD. A strong interaction between the graphene and the incident terahertz wave was expected because of the grating coupler and resonant cavity. The calculated results, including Lorentz conductivity of graphene, agree very well with our experimental results, and the extracted extinction value of the transmission in the resonance frequency is more than 80% at room temperature. Our DC measurement data revealed that a limited frequency range of the graphene plasmon was modulated. A superior graphene plasmon device with a larger frequency variable range may find applications in THz modulators by replacing the top-gate media with stronger sustaining ability and higher gate dielectric capacitance.

References

[1] Chen H T, Padilla W J, Zide Joshua M O, Gossard A C, Taylor A J and Averitt R D 2006 *Nature* **444** 597
[2] Yen T J, Padilla W J, Fang N, Vier D C, Smith D R, Pendry J B, Basov D N and Zhang X 2004 *Science* **303** 1494

[3] Wu H Q, Linghu C Y, Lu H M and Qian H 2013 *Chin. Phys. B* **22** 098106
[4] Ryzhii V 2006 *Jpn. J. Appl. Phys.* **45** 923
[5] Hwang E H and Sarma S D 2007 *Phys. Rev. B* **75** 205418
[6] Yan B, Yang X X, Fang J Y, Huang Y D, Qin H and Qin S Q 2015 *Chin. Phys. B* **24** 015203
[7] Marinko J and Hrvoje B 2009 *Phys. Rev. B* **80** 245435
[8] Ryzhii V, Satou A and Otsuji T 2007 *J. Appl. Phys.* **101** 024509
[9] Grigorenko A N, Polini M and Novoselov K S 2012 *Nat. Photonics* **6** 749
[10] Vicarelli L, Vitiello M S, Coquillat D, Lombardo A, Ferrari A C, Knap W, Polini M, Pellegrini V and Tredicucci A 2012 *Nat. Mater.* **11** 865
[11] Yan B, Fang J Y, Qin S Q, Liu Y T, Zhou Y Q, Li R B and Zhang X A 2015 *Appl. Phys. Lett.* **107** 191905
[12] Marco F, Alexander U, Andreas P, Govinda L, Karl U, Hermann D, Pavel K, Aaron M, Werner S, Gottfried S and Thomas M 2012 *Nano Lett.* **12** 2773
[13] Nicolas U, Iris C, Julien L, Ievgeniia O N, Felix F, Michl K, Thomas S and Alexey B K 2013 *Opt. Express* **21** 24736
[14] Ferrari A C, Meyer J C, Scardaci V, Casiraghi C, Lazzeri M, Mauri F, Piscanec S, Jiang D, Novoselov K S, Roth S and Geim A K 2006 *Phys. Rev. Lett.* **97** 187401
[15] Tu Z Q, Liu Z C, Li Y F, Yang F, Zhang L Q, Zhao Z, Xu C M, Wu S F, Liu H W, Yang H T and Richard P 2014 *Carbon* **73** 252
[16] Lee B, Park S Y, Kim H C, Cho K, Vogel E M, Kim M J, Wallace R M and Kim J 2008 *Appl. Phys. Lett.* **92** 203102
[17] Zhu X L, Yan W Jepsen P U, Hansen O, Mortensen N A Xiao S S, Jackson R and Graham S 2013 *Appl. Phys. Lett.* **102** 131101
[18] Kim S, Nah J, Jo I, Shahrjerdi D, Colombo L, Yao Z, Tutuc E and Banerjee S K 2009 *Appl. Phys. Lett.* **94** 062107
[19] Sambonsuge S, Jiao S, Nagasawa H, Fukidome H, Filimonov S N and Suemitsu M 2016 *Diam. Relat. Mater.* **67** 51